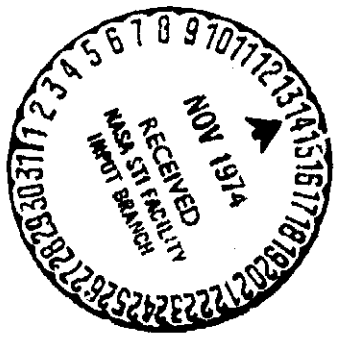

ABSOLUTE SPECTROPHOTOMETRY IN M31 AND M32

J. B. Oke

Hale Observatories, California Institute of Technology

Carnegie Institution of Washington

and

M. Schwarzschild*

Princeton University Observatory

Received: _____

*Visiting Sherman Fairchild Distinguished Scholar,

California Institute of Technology

ABSTRACT

For a number of places in the bulge of M31 and for two places in M32 photometric scans from λ = 3300 Å to λ = 10,600 Å have been obtained with the multichannel spectrometer on the 5-meter Hale telescope. The scans show that in both objects the color temperature (particularly shortwards of 5000 Å) decreases towards the center and that the strength of the CN bands increases towards the center in both objects in agreement with earlier observations. The new data can all be interpreted in terms of an increase of heavy element abundance towards the center in both objects by a factor probably less than 2 and by an excess of heavy elements in M31 compared to M32 by a factor probably greater than 2, in qualitative agreement with earlier conclusions.

Subject Headings: GALAXIES, SPECTROPHOTOMETRY, ABUNDANCES

INTRODUCTION

It has been known for many years that some galaxies show a change of color with distance from the center (Tifft 1961, 1963, de Vaucouleurs 1961, Hodge 1963). Sandage, Becklin, and Neugebauer (1969) have shown that ultraviolet color changes occur in M31 within 20″ of the center. They also report a color change in M32 which depends on distance from the center. The 6-color photometry of Stebbins and Whitford (1948) demonstrated that over a wide spectral range M31 and M32 had different energy distributions. This was also shown by Oke (1962) using detailed scans.

In recent years most of the observational work on M31 and M32 has concentrated on measuring various line strengths or indices to study the metallicity in the objects. We mention as examples the work of McClure and Van den Bergh (1968), McClure (1969), Spinrad and Taylor (1971), Spinrad et al. (1971), Spinrad et al. (1972), Joly and Andrillat (1973).

In order to investigate in more detail the known color changes with distance from the center of M31 and M32, detailed energy distributions covering the wavelength range for λ3300 to λ10,600 have been obtained in the bulge of M31 and at two points in M32. Enough detail is present in some cases to make comments not only on the overall energy distributions but also on the strengths of features such as the CN bands.

OBSERVATIONS

All the observations were made with the multichannel spectrometer attached to the 5-meter Hale telescope. Although the instrument has both a star and sky aperture separated by 40″, this is not useful for sky subtraction in extended objects; hence the instrument was used either without the star-sky chopper running, or by reducing data in the two apertures completely separately. Sky measurements were made well outside of M31 and M32.

It was the original intention to measure separately the tiny 3.″5 diameter nucleus of M31; however, atmospheric refraction effects were too large. All results given in this paper refer to a round aperture of radius 5″. Energy distributions are based on the absolute calibration of α Lyrae as given by Oke and Schild (1970) and results are given in terms of AB = $-2.5 \log f_\nu - 48.60$ when f_ν is the flux in ergs s^{-1} cm^{-2} Hz^{-1}.

The highest resolution measurements, using a bandpass of 40 Å in the blue ($1/\lambda > 1.74$) and 80 Å in the red, are given in table 1. Along with $1/\lambda$, where λ is the wavelength measured in microns, are the fluxes in the center of M31, within a radius of 5″, and the fluxes in a 5″ radius aperture 40″ East of the center. The resulting absolute fluxes, in the form AB, for the

central region are plotted in figure 1a. The difference AB(0-5″) - AB(40″) is in figure 1b. Several of the contributors to strong spectral absorption features are also indicated. Standard deviations are indicated in table 2 where the representative value is tabulated between appropriate values of $1/\lambda$. Standard deviation bars are shown in figure 1 if they are 0.04 mag or larger.

In table 3 are listed the data obtained with bandpasses of 80 Å in the blue ($1/\lambda > 1.74$) and 160 Å in the red. Given in order are (a) observations of the center of M31 within 5″ of the center, (b) measurements made 2′.5 of arc from the center along the major axis toward the Southwest (detailed position in table 2), (c) observations of the center of M32 within 5″ of the center, and (d) measurements of M32 made 40″ East of the center. Standard deviations are again given in table 2. Figure 1c shows the difference in AB for M31 between 40″ and 2′.5. The 40″ data come from table 1 by averaging pairs of measures; additional untabulated measurements made with 80 and 160 Å bands were also incorporated. Figure 1d gives the differences in AB for M32 between the center and 40″ East of the center. The plotted differences cannot be inferred directly from table 3 because the bandpasses for the 40″ data

are displaced 40 Å from those for the center. Interpolations in the 40″ data were accomplished by using the data in table 3 and supplementing it with somewhat less accurate data obtained at the appropriate wavelengths. Difficulties arise only at wavelengths where the fluxes are changing rapidly. Finally figure 1e shows the difference between the central regions of M31 and M32. These data come directly from table 3.

When one tries to make measurement far from the center of M31, the light levels are low. To maintain accuracy a series of measurements closely spaced in time was made with bandpasses of 160 Å in the blue ($1/\lambda > 1.70$) and 360 Å in the red. These were made 40″ East of the nucleus, then 2′.1, 4′.5, 7′.0, and 9′.4 from the nucleus along the major axis defined by a position angle of 37°.7 (de Vaucouleurs 1958) toward the Southwest. Accurate positions are given in table 2. The resulting fluxes are given in table 4 and the standard deviations in table 2. The differences are plotted in figure 2. It should be noted that figures 2a and 1c are nearly comparable, except for spectral resolution.

DISCUSSION

Of all the plots in figures 1 and 2 only plot (a) of figure 1 represents an absolute energy distribution. It simulates the main characteristics of a K-type spectrum,

including the strongest atomic and molecular features which become clearly apparent when 40 and 80 Å bands are used. All the other energy distributions listed in tables 1, 3, and 4 are so similar to the one shown in figure 1a that relevant magnitude differences between them, as given by all the other plots, seem more instructive.

Regarding M31, the following points may be deduced from the figures:

1) Plot (b) of figure 1 shows that the central area compared to an area 40' from the center is redder and has stronger CN blends. The observed changes in CN strength confirms earlier studies (McClure and Van den Bergh 1968, McClure 1969, Spinrad et al. 1972). However, the smallness of the observed differences warrants emphasizing. The strengths of the CN blends in the difference plot (b) are at best one quarter of those in the absolute plot (a). Over the whole spectral range, there is a substantial change in color which arises largely from changes bluewards of λ4200. This is in agreement with the run of U-B and B-V colors given by Sandage, Becklin, and Neugebauer (1969). If for the present purpose a color difference is used based on a 500 Å band centered on 3750 Å ($1/\lambda = 2.67$) and a 1000 Å band centered at 7500 Å ($1/\lambda$ 1.33), one finds from plot (b) a color difference of about 0.15 mag; this may be compared to a corresponding

color difference of about 1.0 mag between a K0 III star and a K3 III star, according to data obtained with the same instrument kindly made available by Dr. J. E. Gunn. Nevertheless, the observed differences between the central area ($r \leq 5''$) and the area at $r = 40''$ seem secure. On the basis of the present observations, it cannot of course be decided how much of the observed difference can be attributed to the nucleus with $r < 1''.6$, (Light et al. 1974) and how much to the annulus between $1''.6$ and $5''.0$. If the nucleus is responsible for the whole effect, the energy distribution of the nucleus will be dramatically different from that of the bulge since it contributes less than 25% of the light within $5''$ of the center.

2) Plot (c) of figure 1 and plot (a) of figure 2 are based on data with insufficient resolution and accuracy to provide critical measures of spectral features. Their accuracy is, however, amply sufficient to show that over the wide wavelength range here covered the area at $r = 40''$ is redder than the areas at $r = 2'.4$ and $r = 2'.1$ (just as had been found for the central area compared to the area at $r = 40''$). Specifically, both plots give a color difference, as here defined, of 0.11 mag, i.e., somewhat smaller than in the preceding comparison. There is some suggestion that changes in the CN band strengths are smaller than in the previous case. On the other hand plot (b) of figure 2 indicates that the energy distributions

in the areas with r = 2'.1 and r = 4'.5 respectively are very nearly identical. Indeed the color difference turns out to be 0.04 mag, hard at the margin of measurability with the present data. Altogether then, these observations give for the entire bulge of M31 a progressive reddening of the spectral gradient as one approaches the center, the spectral changes being minor in the outer portions of the bulge but increasing rapidly towards the center - quite parallel to the strength of the CN features (Spinrad et al. 1971). The values here found for the color difference between the central area and that at r = 2'.4 (i.e., $0^m.15 + 0^m.11 = 0^m.26$) agrees well with earlier corresponding color measurements of $\Delta(U - V) \approx 0.25$ mag (Sandage et al. 1969, Spinrad et al. 1971).

3) The two areas at r = 7'.0 and r = 9'.4 respectively fall outside the bulge of M31 and into the region of the innermost arms. It seems therefore not surprising that plots (c) and (d) of figure 2 show the bulge area at r = 2'.1 to have a redder energy distribution than the two outer areas which presumably contain a substantial fraction of younger Population I stars. The changes in color do not seem to be accompanied by changes in the CN strength.

Regarding M32, the following points may be deduced.

1) Plot (d) of figure 1 shows that M32, just as M31, is redder in its central area than at r = 40", in qualitative

accord with previous measurements (Sandage et al. 1969). The color difference, as here defined, amounts to 0.11 mag. Because of the faintness of M32 at r = 40″, the present data do not suffice for the study of spectral features.

2) Plot (e) of figure 1 reconfirms the well known fact that the center of M31 is redder than that of M32 (Stebbins and Whitford 1948, Oke 1962, Sandage et al. 1969, Spinrad et al. 1971). The color difference, over the present baseline, amounts to 0.35 mag. The same plot also indicates a greater strength of the CN blends in the center of M31 than in that of M32, just as found previously (McClure and Van den Bergh 1968, Spinrad et al. 1972). The difference in CN strengths is larger than the difference between 0-5″ and 40″ in M31.

CONCLUSIONS

Changes in overall color and spectral features can be produced in at least two ways. One of these is by a change in the luminosity function and in particular the relative numbers of cool giants, cool dwarfs, and hotter main sequence and horizontal-branch stars. The second way is by chemical composition differences in different regions. The former will not be discussed since it involves stellar synthesis work. The obvious changes in the CN band strengths relative to the neighboring spectral regions which are affected largely by atomic lines, strongly suggests that abundance differences are indeed important. We can discuss their consequences in more detail.

In terms of the observations presented here, chemical composition changes produce at least <u>two</u> effects.

1) At a constant effective temperature, if the metal abundance is increased, the blue and violet line blanketing increases; the effect is to make the red continuum appear hotter. In cool stars the blue and violet line blanketing is approximately 30 to 40 percent (Oke and Conti 1966), which leads to an apparent temperature increase in the red continuum of about 150° K. This is due to the steepening of the temperature-mean optical depth relation produced by line blanketing. The actual change of blanketing in the blue and violet is estimated by extrapolating the continuum spectrum from $1/\lambda = 1.0$ to 2.0 into the violet, thus producing a speudo-continuum in this spectral range. The estimated apparent changes in effective temperature due to this excess blanketing are

given in column 4, table 5. In two cases from figure 1 the changes are too small to measure adequately.

2) If the dominant stars are giants, an increase in the metal abundance shifts the giant branch to cooler effective temperatures. This changes the overall energy distribution and may change the line blanketing if the line intensities change with temperature.

Since we have energy distributions out to beyond 10,000 Å we can measure accurately temperature differences by measuring the slopes of the energy distribution differences between $1/\lambda = 1.0$ and 2.0, since blanketing is small in this spectral range. The observed changes in slope as derived from figure 1 are listed in column 2 of table 5. To calibrate the change of temperature with slope we can use energy distributions for two giant stars in M67 observed by Gunn (private communication). The stars presumably have the same chemical compositions; they are K0 III and K3 III respectively. The difference in B-V is 0.24 while the difference in slope from $1/\lambda = 1.0$ to 2.0 is 0.42 mag. The difference in effective temperature is about 600° K using Johnson's (1966) calibration. Using these data we calculate from the observed slopes the observed ΔTe in column 3 of table 5. Combining these with the corrections for line

blanketing yields proper values of ΔTe in column 5. They are in the sense, for example, that M31 (0-5') appears cooler than M31 (40').

These temperature differences can be explained if the light comes largely from giants and there are chemical abundance differences. On the basis of extensive new stellar evolution calculations, Drs. A. V. Sweigart, J. G. Mengel and P. G. Gross have kindly informed us that a change in the fractional heavy element abundance by weight, Z, by a factor 2 at Z = 0.02 changes the effective temperature of the giant branch by about 200° K. Accordingly, the ΔTe values listed in the last column of table 5 suggest a) that the heavy element abundance within the bulge of M31 increases towards the center by less than a factor 2, b) that the same is true within M32, and c) that the center of M31 exceeds that of M32 in heavy element abundance by somewhat more than a factor 2.

These conclusions are qualitatively confirmed by the data on the CN features obtained in this investigation. The energy distributions for the two M67 giants observed by Gunn show that over the range of 600° K from K0 III to K3 III, there are essentially no changes in the equivalent widths of the CN bands. Since the temperature differences inferred above are only 350° K or less, temperature differences have practically no effect on the CN bands. This suggests that the observed CN differences are most likely directly caused by chemical abundance differences, as had earlier been deduced by Spinrad and Taylor (1969).

In summary then, the observations here described add further weight to the earlier data indicating an increase of the heavy element abundance towards the center within the bulge of M31 as well as within M32.

This work was supported in part by the National Aeronautics and Space Administration through grant NGL 05-002-134.

REFERENCES

Hodge, P. W. 1963, A. J., 68, 237.

Johnson, H. L. 1966, *Ann. Rev. Astr. and Ap.*, 4, 193.

Joly, M., and Andrillat, Y. 1973, *Astr. and Ap.*, 26, 95.

Light, E. S., Danielson, R. E., and Schwarzschild, M. 1974, Ap. J., 194, 2.

McClure, R. D., and Van Den Bergh, S. 1968, A. J., 73, 313.

McClure, R. D. 1969, A. J., 74, 50.

Oke, J. B. 1962, *Problems of Extra-Galactic Research*, ed. G. C. McVittie (New York: MacMillan Co.) p. 34.

Oke, J. B., and Conti, P. S. 1966, Ap. J., 143, 134.

Oke, J. B., and Schild, R. E. 1970, Ap. J., 161, 1015.

Sandage, A. R., Becklin, E. E., and Neugebauer, G. 1969, Ap. J., 157, 55.

Spinrad, H., and Taylor, B. J. 1969, Ap. J., 157, 1279.

———————————— 1971, Ap. J. Suppl., 22, 445.

Spinrad, H., Gunn, J. E., Taylor, B. J., McClure, R. D., and Young, J. W. 1971, Ap. J., 164, 11.

Spinrad, H., Smith, H. E., and Taylor, D. J. 1972, Ap. J., 175, 649.

Stebbins, J., and Whitford, A. E. 1948, Ap. J., 108, 413.

Tifft, W. G. 1961, A. J., 66, 390.

———————— 1963, A. J., 68, 302.

Vaucouleurs, G. de, 1958, Ap. J., 128, 465.

———————————— 1961, Ap. J. Suppl., 5, 233.

TABLE HEADINGS

TABLE 1

ABSOLUTE FLUXES IN MAGNITUDES AB FOR M31, 40 and 80 Å BANDS

TABLE 2

POSITIONS AND STANDARD DEVIATIONS (IN MAG)

TABLE 3

ABSOLUTE FLUXES IN MAGNITUDES AB, 80 AND 160 Å BANDS

TABLE 4

ABSOLUTE FLUXES IN MAGNITUDES AB FOR M31, 160 AND 360 Å BANDS

(Heading is already on Table 5)

CAPTIONS

Fig. 1.– (a) Absolute spectral energy distribution for the central ($r \leq 5''$) region of M31. The absolute flux AB in magnitudes is plotted against $1/\lambda(\mu)$. A wavelength scale is also plotted along the top of the figure. Strong contributors to the main absorption features are marked. Standard deviation bars are shown if they are $0^m.04$ or larger. (b) The magnitude difference ΔAB between the center ($r \leq 5''$) and a point $40''$ away from the center of M31. (c) Magnitude difference ΔAB between $40''$ and $2'.5$ in M31. (d) Magnitude difference ΔAB between the center ($r \leq 5''$) and a point $40''$ away from the center of M32. (e) Magnitude difference ΔAB between the centers of M31 and M32.

Fig. 2.– Magnitude differences ΔAB as a function of $1/\lambda\ (\mu)$ for different positions in M31. The positions are specified in table 2. Standard deviation bars are shown if $0^m.04$ or larger.

1/λ	$AB_{0-5°}$	$AB_{40°}$	1/λ	$AB_{0-5°}$	$AB_{40°}$	1/λ	$AB_{0-5°}$	$AB_{40°}$	1/λ	$AB_{0-5°}$	$AB_{40°}$	1/λ	$AB_{0-5°}$	$AB_{40°}$
3.085...	14.12	15.55	2.358	12.34	13.82	1.908	11.30	12.82	1.479	10.69	12.20	1.142	9.98	11.50
3.049...	14.03	15.55	2.336	12.38	13.90	1.894	11.24	12.76	1.462	10.64	12.15	1.131	9.93	11.51
3.012...	14.02	15.27	2.314	12.14	13.66	1.879	11.18	12.72	1.445	10.59	12.12	1.121	9.95	11.51
2.975...	14.10	15.43	2.293	12.07	13.60	1.866	11.13	12.67	1.429	10.56	12.09	1.111	9.92	11.50
2.940...	13.98	15.33	2.273	12.05	13.56	1.852	11.17	12.69	1.412	10.56	12.10	1.101	9.85	11.44
2.907...	13.98	15.42	2.252	11.95	13.45	1.838	11.16	12.67	1.396	10.59	12.14	1.092	9.90	11.48
2.874...	13.90	15.29	2.232	11.85	13.35	1.824	11.16	12.68	1.381	10.51	12.08	1.082	9.89	11.46
2.840...	13.80	15.15	2.212	11.81	13.30	1.812	11.12	12.65	1.366	10.42	11.99	1.073	9.96	11.47
2.808...	13.95	15.24	2.193	11.72	13.22	1.799	11.08	12.60	1.351	10.35	11.90	1.064	9.90	11.46
2.778...	13.76	15.12	2.174	11.65	13.18	1.785	11.10	12.61	1.337	10.32	11.85	1.055	9.83	11.39
2.747...	13.50	14.90	2.155	11.66	13.15	1.773	11.07	12.60	1.323	10.30	11.83	1.046	9.79	11.35
2.717...	13.35	14.76	2.136	11.66	13.15	1.761	11.03	12.56	1.309	10.32	11.85	1.037	9.86	11.40
2.687...	13.41	14.85	2.119	11.57	13.08	1.748	11.00	12.54	1.295	10.31	11.84	1.029	9.81	11.36
2.660...	13.54	14.92	2.101	11.51	13.03	1.724	10.94	12.53	1.282	10.33	11.85	1.020	9.79	11.37
2.632...	13.62	14.99	2.083	11.46	12.98	1.701	11.03	12.59	1.269	10.35	11.87	1.012	9.79	11.39
2.603...	13.90	15.22	2.066	11.42	12.94	1.678	10.92	12.42	1.256	10.32	11.84	1.004	9.66	11.26
2.577...	13.53	14.92	2.049	11.46	12.98	1.655	10.86	12.33	1.244	10.25	11.77	0.996	9.63	11.25
2.551...	13.39	14.86	2.033	11.43	12.94	1.634	10.85	12.32	1.232	10.18	11.72	0.988	9.61	11.24
2.525...	13.14	14.61	2.016	11.44	12.92	1.613	10.88	12.36	1.219	10.15	11.72	0.980	9.59	11.16
2.499...	12.66	14.11	2.000	11.50	12.97	1.592	10.85	12.31	1.208	10.11	11.67	0.973	9.58	11.14
2.475...	12.60	14.02	1.984	11.44	12.95	1.572	10.80	12.32	1.196	10.10	11.68	0.965	9.54	11.14
2.451...	12.48	13.91	1.969	11.44	12.98	1.553	10.74	12.29	1.185	10.13	11.62	0.958	9.53	11.19
2.427...	12.53	13.97	1.953	11.44	12.96	1.534	10.71	12.24	1.174	10.17	11.69	0.951	9.54	11.14
2.403...	12.59	13.99	1.938	11.55	13.06	1.515	10.66	12.20	1.163	10.07	11.62	0.943	9.55	11.20
2.380...	12.48	13.92	1.923	11.39	12.93	1.497	10.70	12.22	1.152	10.01	11.58			

Oke & Schwarzschild Table 2

Table	Object	Position	Fractional s.d. between values of 1/λ
1	M31, 0-5′	Centered	3.085(0.04)2.975(0.02)2.747(0.01)0.943
1	M31, 40′	40′E	3.085(0.11)3.012(0.06)2.778(0.04)2.717(0.02)2.499(0.01)1.232(0.02)0.943
3	M31, 0-5′	Centered	3.067(0.03)2.993(0.02)2.793(0.01)0.976(0.02)0.961(0.04)0.933
3	M31, 2′.5	80′W, 126′S	3.067(0.07)2.924(0.03)2.731(0.02)2.512(0.01)1.179(0.02)0.961(0.04)0.933
3	M32, 0-5′	Centered	3.067(0.03)2.993(0.02)2.924(0.01)0.961(0.02)0.933
3	M32, 40′	40′E	3.029(0.09)2.890(0.05)2.762(0.03)2.538(0.02)2.439(0.01)1.214(0.02)1.068(0.04)0.984(0.06)0.940
4	M31, 40′	40′E	2.924(0.02)2.793(0.01)0.921
4	M31, 2′.1	26′W, 127′S	2.924(0.02)2.793(0.01)0.950(0.02)0.921
4	M31, 4′.6	116′W, 249′S	2.924(0.04)2.793(0.02)2.463(0.01)1.018(0.02)0.950(0.03)0.921
4	M31, 7′.0	209′W, 368′S	2.924(0.06)2.793(0.04)2.564(0.02)2.463(0.01)1.196(0.02)0.984(0.03)0.950(0.05)0.921
4	M31, 9′.4	300′W, 477′S	2.924(0.07)2.674(0.04)2.463(0.02)2.370(0.01)1.441(0.02)1.062(0.03)0.950(0.06)0.921

1/λ	M31 0-5°	M31 2.5	M32 0-5°	1/λ	M32 40°	1/λ	M31 0-5°	M31 2.5	M32 0-5°	1/λ	M32 40°
3.067...	14.14	16.68	13.42	3.029	17.22	1.736	11.02	13.89	10.71	1.779	14.95
2.993...	14.08	16.69	13.30	2.959	17.43	1.689	11.01	13.90	10.71	1.754	14.93
2.924...	13.98	16.55	13.25	2.890	17.23	1.644	10.82	13.64	10.52	1.730	14.86
2.856...	13.85	16.44	13.17	2.825	17.08	1.602	10.84	13.66	10.55	1.706	14.90
2.793...	13.88	16.47	13.17	2.762	17.05	1.562	10.78	13.62	10.49	1.666	14.75
2.731...	13.43	16.11	12.84	2.703	16.93	1.524	10.70	13.54	10.45	1.623	14.71
2.674...	13.55	16.06	12.89	2.646	16.93	1.488	10.66	13.51	10.39	1.582	14.67
2.617...	13.78	16.33	12.97	2.591	16.92	1.453	10.60	13.45	10.36	1.543	14.56
2.564...	13.48	16.16	12.84	2.538	16.74	1.420	10.55	13.41	10.28	1.506	14.55
2.512...	12.85	15.54	12.32	2.488	16.19	1.389	10.57	13.43	10.32	1.471	14.51
2.463...	12.52	15.23	12.02	2.439	16.12	1.358	10.38	13.25	10.14	1.437	14.55
2.415...	12.57	15.26	11.96	2.392	16.02	1.330	10.28	13.15	10.09	1.404	14.55
2.370...	12.42	15.17	11.91	2.347	16.04	1.275	10.33	13.20	10.10	1.374	14.39
2.325...	12.28	15.04	11.83	2.304	15.85	1.250	10.29	13.15	10.09	1.344	14.30
2.283...	12.08	14.87	11.67	2.262	15.72	1.225	10.15	13.02	9.93	1.316	14.25
2.242...	11.91	14.70	11.49	2.222	15.57	1.202	10.08	12.96	9.92	1.289	14.24
2.203...	11.78	14.58	11.40	2.183	15.47	1.179	10.18	13.05	9.98	1.263	14.24
2.164...	11.66	14.48	11.27	2.146	15.42	1.157	10.09	12.92	9.93	1.238	14.16
2.128...	11.64	14.42	11.26	2.110	15.35	1.136	9.94	12.86	9.76	1.214	14.07
2.092...	11.51	14.31	11.12	2.075	15.29	1.116	9.93	12.84	9.79	1.190	14.14
2.058...	11.46	14.28	11.14	2.041	15.28	1.077	9.92	12.77	9.76	1.168	14.10
1.960...	11.46	14.26	11.06	2.008	15.22	1.059	9.93	12.83	9.74	1.147	14.03
1.931...	11.49	14.27	11.09	1.976	15.23	1.041	9.84	12.75	9.65	1.126	13.95
1.901...	11.27	14.06	10.94	1.946	15.20	1.024	9.80	12.70	9.65	1.106	13.93
1.873...	11.17	13.99	10.87	1.916	15.14	1.008	9.69	12.57	9.53	1.087	13.95
1.845...	11.18	13.99	10.85	1.887	15.04	0.992	9.62	12.55	9.52	1.068	13.88
1.818...	11.17	13.98	10.85	1.859	15.00	0.976	9.55	12.47	9.42	1.050	13.95
1.792...	11.09	13.89	10.77	1.832	14.97	0.961	9.52	12.49	9.41	1.033	13.96
1.767...	11.07	13.90	10.77	1.805	14.89	0.933	9.44	12.44	9.35	1.016	13.82
										1.000	13.73
										0.984	13.74
										0.969	13.62
										0.954	13.65
										0.940	13.60

Oke & Schwarzschild Table 3

Oke & Schwarzschild Table 4

$1/\lambda$	40″	2′.1	4′.5	7′.0	9′.4
2.924...	15.18	16.35	17.45	17.95	18.12
2.793...	14.98	16.20	17.13	17.65	17.96
2.674...	14.76	15.97	16.93	17.48	17.80
2.564...	14.70	15.91	16.85	17.34	17.69
2.463...	13.82	15.10	16.04	16.57	16.96
2.370...	13.76	15.01	15.96	16.49	16.86
2.283...	13.40	14.69	15.64	16.21	16.56
2.203...	13.13	14.41	15.35	15.92	16.28
2.128...	13.01	14.30	15.27	15.82	16.19
2.058...	12.89	14.18	15.15	15.72	16.06
1.992...	12.85	14.16	15.13	15.67	16.04
1.931...	12.82	14.11	15.07	15.64	15.99
1.873...	12.59	13.90	14.87	15.45	15.81
1.818...	12.54	13.86	14.81	15.40	15.73
1.767...	12.49	13.80	14.77	15.35	15.71
1.718...	12.42	13.73	14.68	15.27	15.63
1.608...	12.30	13.62	14.59	15.19	15.55
1.529...	12.15	13.47	14.44	15.03	15.38
1.441...	12.11	13.42	14.41	14.99	15.36
1.377...	12.04	13.37	14.35	14.95	15.35
1.305...	11.72	13.05	14.02	14.63	15.00
1.250...	11.67	12.99	13.96	14.59	14.93
1.196...	11.58	12.90	13.88	14.50	14.88
1.146...	11.48	12.80	13.78	14.40	14.78
1.102...	11.39	12.74	13.69	14.34	14.70
1.062...	11.35	12.71	13.66	14.30	14.52
1.018...	11.23	12.55	13.50	14.17	14.61
0.984...	11.12	12.44	13.40	14.16	14.48
0.950...	11.04	12.36	13.36	14.08	14.40
0.921...	10.70	12.09	13.01	13.73	13.94

TABLE 5

EFFECTIVE TEMPERATURE DIFFERENCES

Pairs of Objects	ΔAB ($1/\lambda$=1.0 to 2.0)	Observed ΔTe (° K)	Blanketing Correction (° K)	True ΔTe (° K)
M31(0-5″)-M31(40″)....	-0.04	-60	-40	-100
M31(40″)-M31(2′.5).....	-0.03	-40	small	-40
M31(0-5″)-M32(0-5″)...	-0.20	-290	-60	-350
M32(0-5″)-M32(40″)....	-0.04	-60	small	-60

Oke & Schwarzschild Fig. 1

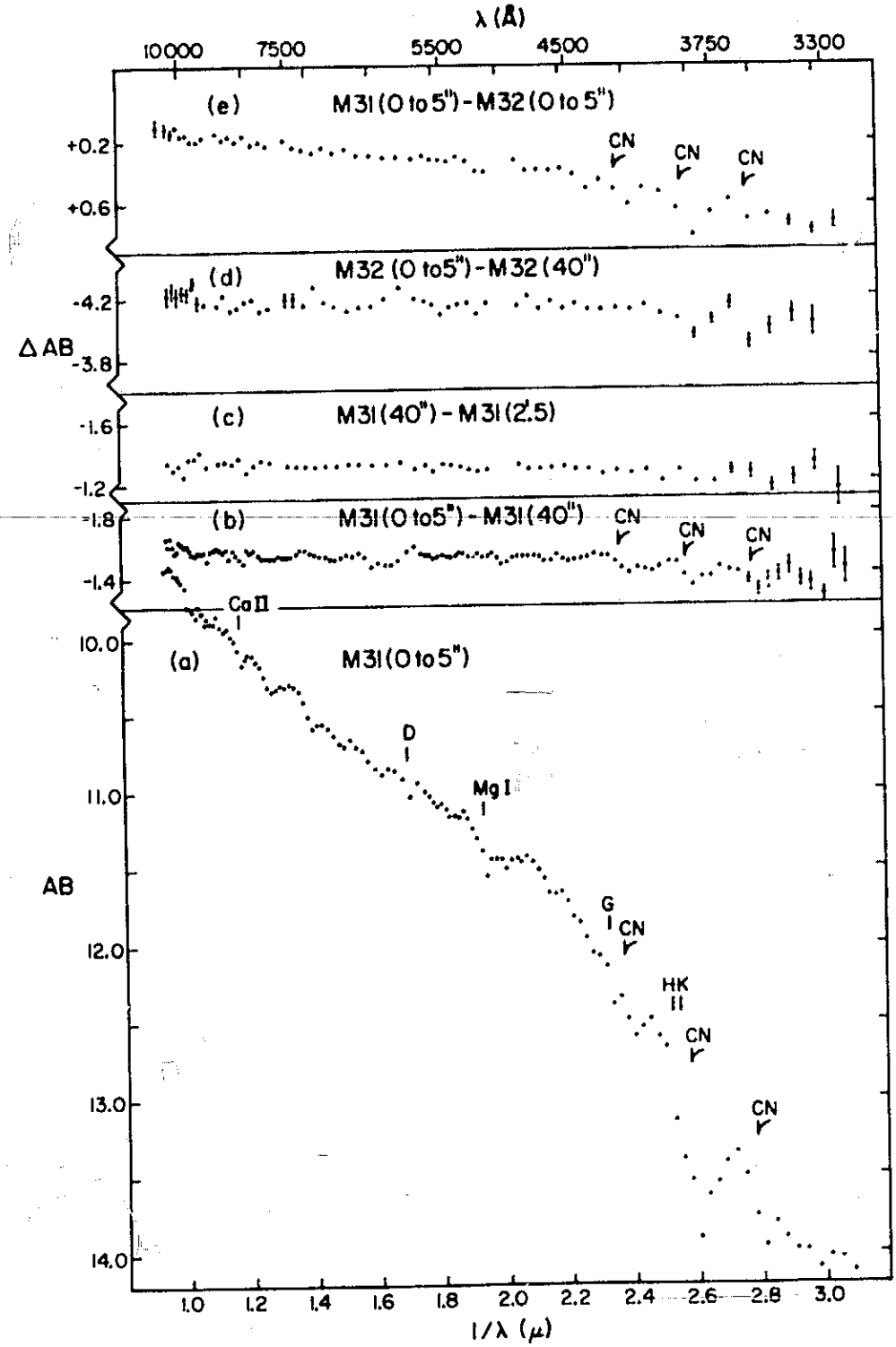

Oke & Schwarzschild Fig 2.

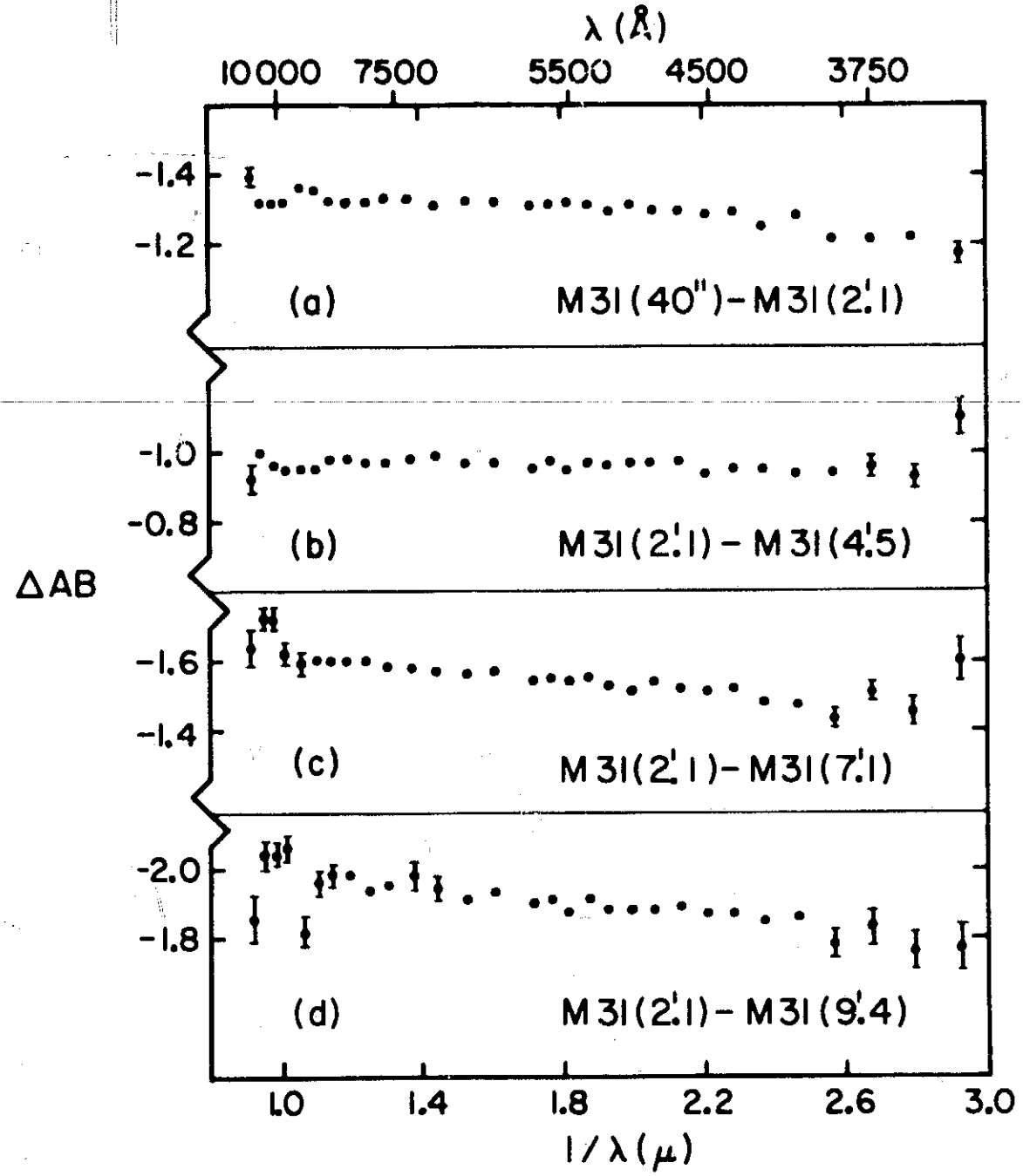

Authors' addresses:

J. B. Oke, California Institute of Technology, Mail Code 105-24, 1201 E. California Boulevard, Pasadena, CA 91125;

M. Schwarzschild, Princeton University Observatory, Peyton Hall, Princeton, N.J. 08540.